ETH
Eidgenössische Technische Hochschule Zürich
Swiss Federal Institute of Technology Zurich

Technical University of Denmark
DTU

Management and Control

Balancing Power in the European System (BPES)

Report on Work Package 4

EEH – Power Systems Laboratory
Swiss Federal Institute of Technology (ETH) Zurich

CEE – Center for Electrical Engineering
Technical University of Denmark (DTU) Copenhagen

Authors and Contact

Matthias Bucher	Power Systems Laboratory, ETH Zurich	mb@eeh.ee.ethz.ch
Göran Andersson	Power Systems Laboratory, ETH Zurich	andersson@eeh.ee.ethz.ch
Stefanos Delikaraoglou	Center for Electrical Engineering, DTU Copenhagen	stde@dtu.dk
Kai Heussen	Center for Electrical Engineering, DTU Copenhagen	kh@dtu.dk

Executive Summary

The goal of this report is to present and explain the main features of the methodologies developed within the BPES project focusing on the management and control of the European power system during balancing operation. These methods build upon the characterization and modelling approaches presented in the work package 2 report [1].

The methodologies presented here aim to address different aspects of balancing operation primarily related with the issues of balancing operation and market, the operational flexibility and the uncertainty due to the stochastic infeed of renewable energies.

This report is organized in five parts, each one describing the main components of the proposed methodologies and some illustrative examples. A thorough presentation and discussion of the results from case studies are included in work package 5 report [2].

The first part focuses on the topic of *spatio-temporal coupling of infeed uncertainties* providing a methodology to generate statistical scenarios that accurately represent the space-time correlations, based on state-of-the-art forecasting methodologies. These scenarios can be readily used as input to decision-making tools related to power system operation and economics.

The interrelated topics of operational flexibility and uncertainty are discussed in the second part. We propose a unified framework that allows to characterize and quantify these two concepts using the same metric. In part III, this framework is integrated in the operational strategy of the system operator. This *new balancing mechanism* employs a robust optimization approach to guarantee sufficient level of reserves with minimum cost for the worst case realization of the uncertainty. In addition, this part addresses the topics of *locational flexibility* where the effect of limited transmission capacity on the operational flexibility is explicitly considered. In a similar vein, the topic of cross-border and temporal coordination between different regions and trading floors, respectively, is addressed showing the benefits of dynamic transmission capacity allocation in the absence of adequate intraregional market coordination.

Unlike current balancing schemes that focus mainly on the reactive dispatch of control reserves, in part IV we propose an approach of *predictive dispatch* that optimally prepositions the balancing resources in anticipation of uncertainty. In addition, we formulate a methodology that enables the efficient *inter-TSO coordination* based on the exchange of a minimal amount of information for their internal power system.

Finally, in the fifth part of this report we focus on operational and grid expansion models that explicitly consider the *transmission side flexibility* brought into the system using dynamic line rating (DLR) or HVDC interconnections. The DLR capabilities are taken into account during the reserve procurement phase based either on a centralized approach (robust optimization) or decentralized policies.

Contents

Chapter 1

Introduction

This report aims to provide an outline of the main methods developed within the BPES project framework regarding the management and control of the European power system with emphasis on balancing operation. The methodological approaches presented in the subsequent chapters follow the characterization and modeling principles and approaches described in the report of work package 2 [1].

The proposed methods aim to contribute towards three main pillars relevant in the context of balancing as shown in Fig. 1.1, namely the *balancing operation and market*, the *operational flexibility* and the *uncertainty* introduced mainly by fluctuations and forecast errors of the variable renewable energy generation.

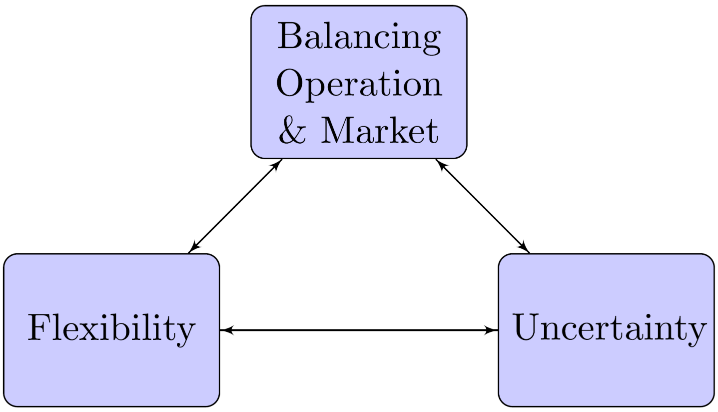

Figure 1.1: Three main pillars of methodological contribution of this report.

The report consists of five main parts focusing on different aspects related with power system balancing. Each chapter includes an introductory part describing the motivation and the basic idea of the corresponding method which is then explained using the main equations and mathematical formulation. Finally, the applicability of each method is illustrated based on selected examples. A detailed presentation of the results along with an in-depth discussion are provided in the report of work package 5 [2].

The first part provides an overview of state-of-the-art forecasting methodologies to generate different types of forecasts, i.e., point and probabilistic predictions as well as spatio-temporal scenarios, in order to describe wind power uncertainty. This is a generic framework that can be also applied to describe different sources of uncertainty, e.g., load or PV production. In order to include these high-quality forecasts in the decision-making process of the system operator a stochastic unit commitment model is formulated as a two-stage optimization problem considering day-ahead and expected real-time dispatch.

The second part deals with the characterization of operational flexibility of the power system. Starting from concrete definitions of operational and locational flexibility, we outline a methodology that permits to describe flexibility and uncertainty in a unified framework based on the trinity of ramping, power and energy. In addition, we present an uncertainty characterization approach which is able to capture the spatio-temporal structure of forecast errors over multiple time-steps. Hence, this method allows a direct comparison of these values and consequently the assessment of secure power system operation.

The third part of the report focuses on alternative procurement reserve strategies in view of power system's flexibility and the available transmission capacity. In particular, we formulate a procurement algorithm that incorporates a probabilistic power flow taking into account the uncertainty of forecast errors, the influence of manual and automatic control reserves as well as the properties of HVDC transmission. Another approach for the procurement of control reserves is based on a robust optimization problem that finds the least-cost reserves for the worst-case realization of the uncertainty following the definitions provided in part II. Finally, we evaluate the efficiency of different market-clearing algorithms for the settlement of reserve capacity, day-ahead and balancing markets in systems with high shares of renewables and we analyse the effect of the explicit transmission allocation on the expected system cost.

Part IV concentrates on the activation and coordination of reserves. A methodological framework for the definition and the evaluation of predictive dispatch is outlined describing the main parameters of operational strategies and their mathematical formulation. The inter-TSO coordination approach determines the bounds on the possible tie-line flow changes as an information proxy for the allowed re-dispatch actions of the neighbouring power systems without revealing any sensible information about the domestic system state.

Finally, part V targets the problem of grid expansion considering operational flexibility aiming to incorporate Dynamic Line Rating in the decision-making of the system operators. In addition, an optimization-based methodology that finds optimal placements of the terminals of the HVDC overlay grid is presented considering both economic and improved controllability features of this transmission technology.

Part I

Wind Power Forecasting Methodologies

1.1 Motivation

The existing market architecture, i.e., sequential clearing of the day-ahead and real-time markets, serves the requirements of a power system based on conventional generation where dispatch decisions need to be planned ahead and the balancing operation is driven by discrete disturbances that cannot be predicted in advance, e.g., outages of generators or transmission lines. However, the efficiency of this market design is disputed as the shares of intermittent renewables increase.

In order to account for the flexibility needs of the power system and take advantage of the - even partial - predictability of wind power, stochastic optimization models are gaining increased attention. Nevertheless, stochastic programming presents a significant challenge regarding the uncertainty modeling in terms of scenarios, since their quality affects considerably the outcome of these models.

Most of the existing wind power prediction tools produce deterministic forecasts [3], which provide only a single value about the expected wind power. Recent research has also focused on probabilistic predictions [4], [5], giving the overall probability distribution of the power output and enabling the estimation of the marginal uncertainty, i.e., the probability distribution of prediction errors. However, probabilistic forecasts are still unable to model the development of these errors in space and in time. To capture this information, it is necessary to generate scenarios that respect both the spatial [6] and the temporal [7] interdependence structure of the forecast errors. These scenarios are suitable to be used in a stochastic optimization framework.

Here we provide a methodological framework that describes the stochastic processes pertaining to wind power at different locations and forecast lead times. Wind power uncertainty is characterized in form of:

1. point forecasts
2. probabilistic predictions and
3. spatio-temporal scenarios of short-term wind power production.

1.2 Main idea and method

This section provides an outline of the methodology used to generate different types of wind power forecasts. Single valued predictions (point forecasts) are produced using a Support Vector Regression (SVR) approach. Based on these point predictions, nonparametric probabilistic predictions are issued and their marginal distributions are retrieved. Finally, spatio-temporal wind power scenarios are obtained using Monte-Carlo sampling techniques.

1.2.1 Support vector regression for short-term power predictions

A powerful technique for forecasting applications is support vector regression (SVR), which is based on kernel regression and belongs to the family of machine learning methods. In case of wind power forecasting, the goal of the SVR algorithm is to find a direct mapping of wind speed on produced wind power. Let $p_{s,t}$ the actual wind power production at time t and location s, and $\hat{p}_{s,t+k|t}$, $\hat{u}_{s,t+k|t}$ the wind power and the speed forecasts respectively, issued at time t with leading horizon $h_k = 1, ...k, ..., d_k$. The SVR model aims to find a prediction function $\hat{g} : \mathbb{R}^u \times \mathbb{R}^h \times \mathbb{R}^p \to \mathbb{R}$ such that $\hat{p}_{s,t+k|t} = \hat{g}(\hat{u}_{s,t+k|t}, h_k, p_{s,t})$.

For a given set of training data $(\theta_1, \nu_1), \dots, (\theta_i, \nu_i), \dots, (\theta_n, \nu_n)$, where $\theta_i \in \Theta$ are the input patterns and ν_i the corresponding output values, the SVR algorithm finds a function $g(\theta)$ whose deviation from the actually obtained targets ν_i is less or equal to a predetermined non-negative value ε.

Assuming that $g(\theta)$ is a of the form $g(\theta) = \langle w, \theta \rangle + b$, $w \in \mathcal{W}, b \in \mathbb{R}$, the mathematical formulation of the optimization problem that SVR solves is

$$\min_{w,b,\xi,\xi^*} \quad \frac{1}{2}\|w\|^2 + C\sum_{i=1}^{n}(\xi_i + \xi_i^*) \quad \text{s.t.} \tag{1.1}$$

$$\nu_i - \langle w, \theta_i \rangle - b \leq \varepsilon + \xi_i \tag{1.2}$$

$$\langle w, \theta_i \rangle + b - \nu_i \leq \varepsilon + \xi_i^* \tag{1.3}$$

$$\xi, \xi^* \geq 0 \tag{1.4}$$

where $\|w\|$ is the Euclidean norm defining the flatness of the regression function and $\langle \cdot, \cdot \rangle$ the dot product in the space of the input patterns $\mathcal{W}$. It holds that $\|w\|^2 = \langle w, w \rangle$. The slack variables ξ_i and ξ_i^* are used in order to relax the constraints related to the ε-insensitive region, such as only the points that are located outside this region are penalized [8].

The objective function (1.1) consists of two terms. The first term, $\frac{1}{2}\|w\|^2$, represents the degree of complexity, i.e., the flatness of the function. The second term, $\sum_{i=1}^{n}(\xi_i + \xi_i^*)$, corresponds to the tolerance for deviations larger than ε. The manually adjustable constant C determines the trade-off between these two properties of the function.

In cases where the dimensionality of w is much higher than the number of observations as well as in order to extend the SVR algorithm to non-linear functions, it is useful to solve the dual formulation of the problem (1.1)-(1.4) [8]. The dual formulation of the problem as well as extensions to non-linear regression functions are explained in detail in [9].

1.2.2 Probabilistic forecasts using nonparametric probabilistic distributions

Probabilistic forecasts are considered in form of nonparametric predictive densities, where the cumulative distribution functions of wind power production are described by a set of quantile forecasts. Being at time t and for location s, write $\hat{f}_{s,t+k|t}$ the probabilistic forecast of the density function of wind power production $p_{s,t+k}$ at time $t+k$ and $\hat{F}_{s,t+k|t}$ the corresponding cumulative distribution function. Given that $\hat{F}_{s,t+k|t}$ is a strictly increasing function, every quantile $\hat{q}^{(\alpha_i)}_{s,t+k|t}$ with nominal proportion α_i, i.e., the predicted power value which has probability α_i to cover the observation, is uniquely defined as

$$\hat{q}^{(\alpha_i)}_{s,t+k|t} = \hat{F}^{-1}_{s,t+k|t}(\alpha_i). \tag{1.5}$$

Consequently, a nonparametric forecast $\hat{F}_{s,t+k|t}$ can be assembled as

$$\hat{F}_{s,t+k|t} = \left\{ \hat{q}^{(\alpha_i)}_{s,t+k|t} | 0 \leq \alpha_1 < ... < \alpha_i < ... \leq 1 \right\}. \tag{1.6}$$

The quantile regression model employed in this work is based on the methodology described in [10]. For a training set of data $(\hat{p}_{s,t+k|t}, p_{s,t+k})$, each quantile $\hat{q}^{(\alpha_i)}$ is calculated by a parametric polynomial function $\eta(\hat{p}_{s,t+k|t}, \boldsymbol{\beta}^{(\alpha_i)})$, where $\boldsymbol{\beta}^{(\alpha_i)}$ is a vector of model parameters, estimated by solving the following optimization problem

$$\hat{\boldsymbol{\beta}}^{(\alpha_i)} = \arg\min_{\boldsymbol{\beta}} \sum_{i=1}^{n} \rho_{\alpha_i}(p_{s,t+k} - \eta(\hat{p}_{s,t+k|t}, \boldsymbol{\beta}^{(\alpha_i)})). \tag{1.7}$$

In the above formulation ρ_{α_i} is the tilted absolute function defined as

$$\rho_{\alpha_i}(u) = u(\alpha_i - \mathbb{1}(u < 0)). \tag{1.8}$$

Figure 1.2 depicts an example of probabilistic predictions along with the corresponding point forecasts and the actual measurements (Data sources are described in [9]).

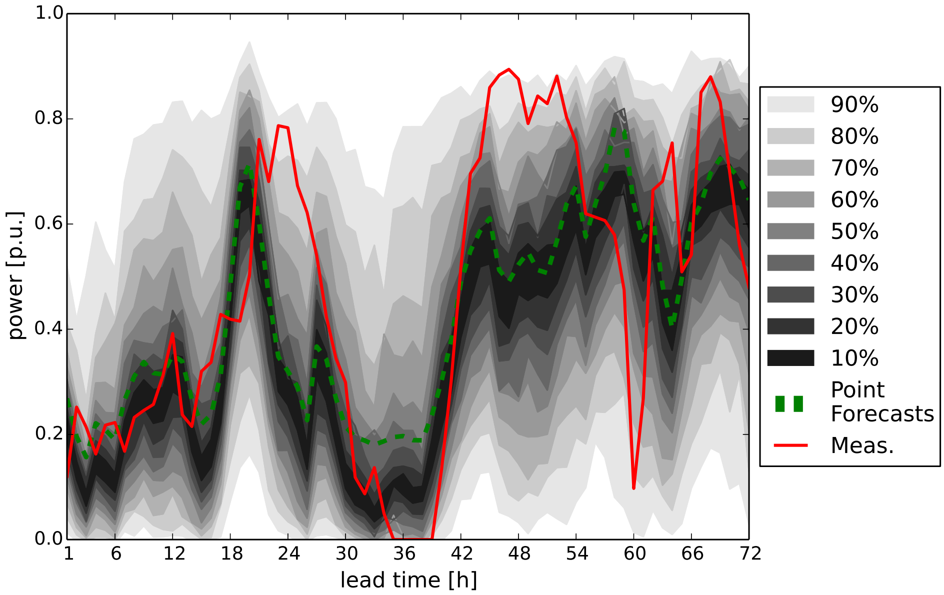

Figure 1.2: Nonparametric probabilistic forecasts of wind power production with nominal coverage rates of the prediction intervals 10, 20,..., and 90%, produced with quantile regression, accompanied with the corresponding point forecasts and measurements.

1.2.3 Spatio-temporal scenarios of wind power generation

Aiming to produce wind power scenarios that respect the spatio-temporal interdependence structure of the forecast errors, we employ an extended version of the method presented in [7] and [6] which focus solely on the temporal and spatial dependencies, respectively.

Denoting by d_s and d_k the number of locations and lead times respectively, the overall dimension of the scenario generation problem is $d = d_s \times d_k$. Assuming that the spatio-temporal dependence structure can be modeled by a Gaussian copula, the covariance matrix $\mathbf{\Sigma} \in \mathbb{R}^{d \times d}$ of a d-dimensional standard normal random variable $\mathbf{X}_t \sim \mathcal{N}_d(0, \mathbf{\Sigma})$ fully captures the interdependence structure, for all lead times and locations. Given the assumption of the Gaussian meta-model, the diagonal elements of $\mathbf{\Sigma}$ are equal to 1, while the off-diagonal elements represent the correlation between the corresponding random variables.

Write $Y_{s,k}$ the random variable whose realization at time t is defined as

$$Y_{s,k}^{(t)} = \hat{F}_{s,t+k|t}(p_{s,t+k}), \quad \forall t, \forall s, \forall k \tag{1.9}$$

and follows a uniform distribution, $Y_{s,k} \sim \mathcal{U}\,[0, 1]$. Then, a standard normal random variable $X_{s,k} \sim \mathcal{N}\,(0, 1)$ is obtained using the following transformation

$$X_{s,k}^{(t)} = \Phi^{-1}\left(Y_{s,k}^{(t)}\right), \quad \forall t, \forall s, \forall k \tag{1.10}$$

where Φ^{-1} is the inverse of the Gaussian cumulative distribution function. Applying this transformation into all uniform variables $Y_{s,k}^{(t)}$, for all the locations and lead times, one obtains d standard Gaussian variables, whose multivariate structure is described by $\mathbf{\Sigma}$. The covariance matrix $\mathbf{\Sigma}$ is estimated based on historical data (i.e., a training period with $t = 1, \ldots, \tilde{T}$) using the following expression

$$\mathbf{\Sigma} = \sum_{t=1}^{\tilde{T}} \mathbf{X}_t \mathbf{X}_t^\top \tag{1.11}$$

where

$$\mathbf{X}_t = \begin{pmatrix} \Phi^{-1}\left(\hat{F}_{s_1,t+1|t}(p_{s_1,t+1})\right) \\ \cdots \\ \Phi^{-1}\left(\hat{F}_{s_1,t+d_k|t}(p_{s_1,t+d_k})\right) \\ \vdots \\ \Phi^{-1}\left(\hat{F}_{s_{d_s},t+1|t}(p_{s_{d_s},t+1})\right) \\ \cdots \\ \Phi^{-1}\left(\hat{F}_{s_{d_s},t+d_k|t}(p_{s_{d_s},t+d_k})\right) \end{pmatrix} \tag{1.12}$$

is the vector of previous measurements transformed through the probabilistic forecast series issued at time t and the probit function Φ^{-1}. In practical applications the covariance matrix can be adaptively estimated using a recursive estimation method as discussed in [7]. In order to ensure that $\mathbf{\Sigma}$ is a suitable covariance matrix of a unit multivariate Normal variable, the following transformation is applied

$$\mathbf{\Sigma}^{\text{calib}} = \mathbf{\Sigma} \oslash (\boldsymbol{\sigma}_t \boldsymbol{\sigma}_t^\top) \tag{1.13}$$

to calibrate the initial covariance matrix, where $\boldsymbol{\sigma}_t$ is the vector of standard deviations and $\oslash$ denotes the element-by-element division.

For the generation of a set of Ω spatio-temporal scenarios, a multivariate Normal random number generator with zero mean and covariance matrix $\mathbf{\Sigma}^{\text{calib}}$ is used to draw Ω realizations of $\mathbf{X}_t$. Then, for every lead time and every location, the inverse probit function Φ is applied to each element $X_{s,k}^{(\omega)}$ of $\mathbf{X}_t$ in order to obtain Ω realizations of $Y_{s,k}^{(\omega)}$ as

$$Y_{s,k}^{(\omega)} = \Phi(X_{s,k}^{(\omega)}) \;\; \forall s, \forall k, \forall \omega \tag{1.14}$$

Finally, the trajectories of wind power generation that respect the predictive densities of the probabilistic forecasts are obtained using the following transformation

$$\hat{p}^{(\omega)}_{s,t+k|t} = \hat{F}^{-1}_{s,t+k|t}(Y^{(\omega)}_{s,k}) \quad \forall s, \forall k, \forall \omega. \tag{1.15}$$

The set of the above transformations for the random variable p can be summarized as follows:

$$\hat{F}(p) = Y \sim \mathcal{U} \Leftrightarrow \Phi^{-1}(Y) = X \sim \mathcal{N} \Leftrightarrow \Phi(X) = Y \Leftrightarrow \hat{F}^{-1}(Y) = p \tag{1.16}$$

Figure 1.3 shows an example of space-time scenarios of short-term wind power production for the same episode as Fig. 1.2.

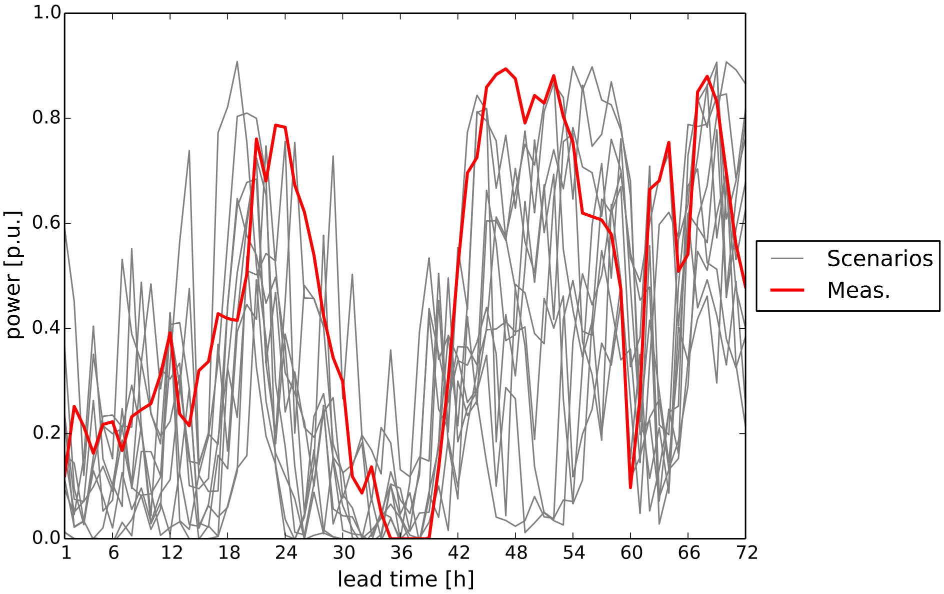

Figure 1.3: Example of 10 spatio-temporal scenarios of wind power production (for the same period and location as in Fig. 1.2).

The rest of the chapter outlines the main structure of a stochastic unit commitment model and the results from its application on an illustrative 14-bus system. Further details about the complete mathematical formulation as well as the data of the case study can be found in [9].

1.2.4 Stochastic Unit Commitment

In order to demonstrate the applicability of the wind power forecasts on power system and electricity market studies, we consider the following two-stage stochastic unit commitment model, where the first stage represents the day-ahead schedule and the second stage represents the real-time dispatch, i.e, the decisions which can be modified once the uncertainty is revealed.

This optimization model is a mixed integer linear programming problem (MILP) due to the binary variables modeling the on/off status of the generators.

A compact version of the stochastic unit model is written as:

$$\underset{\Theta_1}{\text{Minimize}} \quad C^D(p_G, p_W, u) + \mathbb{E}\left[C^B(y_\omega)\right] \tag{1.17}$$

s.t.

$$h^D(p_G, p_W, \delta^0) - L = 0 \tag{1.18}$$
$$g_1^D(u) \leq 0 \tag{1.19}$$
$$g_2^D(\delta^0) \leq T \tag{1.20}$$
$$p_W \leq \overline{W} \tag{1.21}$$
$$h^B(y_\omega, \delta^0, \delta_\omega) + W_\omega - p_W = 0, \quad \forall \omega \in \Omega \tag{1.22}$$
$$g_1^B(p_G, y_\omega, u) \leq 0, \quad \forall \omega \in \Omega \tag{1.23}$$
$$g_2^B(y_\omega) \leq 0, \quad \forall \omega \in \Omega \tag{1.24}$$
$$g_3^B(\delta_\omega) \leq T, \quad \forall \omega \in \Omega \tag{1.25}$$
$$u \in \{0, 1\} \tag{1.26}$$

where $\Theta_1 = \{p_G, p_W, \delta^0, \delta_\omega, y_\omega, u\}$ is the set of vectors of optimization variables.

The objective function (1.17) aims to minimize the expected cost of power system which is made up of the day-ahead and the balancing cost components. The day-ahead cost includes the energy production (p_G, p_W) for conventional and wind power units respectively, the start-up and the shutdown costs (given by the on/off status u of each unit). In real-time operation additional costs arise from the balancing actions y_ω (reserve deployment , wind power spillage and load shedding).The proposed model considers the technical limits of the conventional and wind power units both in day-ahead scheduling (constraints (1.19),(1.21)) and real-time operation (constraints (1.23), (1.24)). In addition, transmission capacity constraints are included through (1.20) and (1.25). Equations (1.18) and (1.22) enforce the power balance at every grid node at day-ahead and real-time stage respectively.

1.3 Potential and Limitations

The wind power forecasting methodologies presented in this section are considered state-of-the-art approaches for producing high quality wind power forecasts. The methodological framework outlined here, allows to produce different types of forecasts, i.e., point predictions, probabilistic forecasts and spatio-temporal scenarios, which can be used as inputs in a variety of power system and electricity market studies, depending on the preferred optimization techniques, e.g., deterministic or stochastic optimization.

These forecasting techniques can be applied into operational problems given the availability of reliable wind speed forecasts and complete information about the technical characteristics of the wind farms deployed in the system. Additional computational complexity regarding both the generation of spatio-temporal scenarios and the solution of the stochastic unit commitment model may arise if the number of wind farm locations and forecast lead-times becomes quite large.

Part II

Characterization of Operational Flexibility

Introduction to operational flexibility

This part focuses on the characterization of two important system properties, namely *flexibility* and *uncertainty*, using a unified framework that enables their comparison. For the scope of the following chapter we define the following terms:

Definition 1 *Operational flexibility is the capability of the power system to follow a schedule that continuously attains active power balance and to contain infeed deviations from this schedule in order to maintain a secure operating state.*

On the previous definition, the term *schedule* refers to the result of an operational planning process, e.g., a market-clearing, that takes into consideration the availability of generation/demand resources and their economic constraints. Infeed deviations refer to unscheduled changes in the net nodal power injections within a timeframe from hours up to the order of several seconds, e..g, due to wind power forecast errors.

In this context the notion of security relates to the definition provided in [11]: *Security* of a power system refers to the degree of risk in its ability to survive imminent disturbances (contingencies) without interruption of customer service. It relates to robustness of the system to imminent disturbances and, hence, depends on the system operating condition as well as the contingent probability of disturbances.

As operational flexibility may differ depending on the grid location and the current network utilization, we introduce the term *locational flexibility* as:

Definition 2 *Locational flexibility is the operational flexibility available at a given bus in the grid.*

In other words, it describes the size of a disturbance at a specific node that could be contained by suitable and available remedial actions. These actions comprise re-dispatching measures such as deployment of reserves, demand side participation as well as changes in network topology and power flow set-points.

The first section describes a method to assess the locational flexibility available in every grid location, based on the projection of the *flexibility set* on the axes of the local disturbance. The second section outlines a method that allows to express uncertainty in the same metrics as flexibility and can be interpreted as the uncertainty budget of the power system over multiple time-steps.

Chapter 2

Characterization of Locational Flexibility

2.1 Motivation

For a TSO the characterization of flexibility, i.e. a measure to describe disturbances that can be balanced, is essential. Based on a metric, TSO might identify critical grid situations, such as high ramping requirements during certain periods of day (e.g. a phenomenon the Californian TSO describes as *duck curve* is caused by the large deployment of PV installations which reduce power output while the evening peak builds up). Different metrics have been described but, to the best of our knowledge, none includes transmission constraints which results in locally different flexibility availability, i.e. locational flexibility. In this section we present how a particular flexibility metric can be extend to incorporate grid constraints. The resulting so called *flexibility set* will be used in chapter 5 in a procurement mechanism.

2.2 Main idea and method

The flexibility metric used in the following method is based on [12] and comprises a trinity consisting of ramping rate ($\frac{MW}{min}$), power capacity (MW) and energy (MWh). For system-wide aggregations of unit's individual flexibility, this metric has been extensively studied, e.g. [13], [14], [12].

The determination of locational flexibility is based on the fact that in order to cover a disturbance at some location in the grid, the locally accessible flexibility needs to be at least as large as the disturbance. It follows four steps:

1. Determining each unit's individual flexibility based on the given system state, i.e. dispatch.

2. Attach (unconstrained) virtual disturbances to the nodes where uncertainty of interest.

3. Impose system-wide coupling constraints, such as active power balance and transmission constraints. The virtual disturbances are considered in the coupling constraints.

4. Formulate the flexibility set by stacking all the constraints to a linear matrix inequality. The flexibility set takes the form as in Eq. (2.1). All δ for which this equation holds, the system is able balance the disturbance. The flexibility set comprises constraints for the generation units, ramping limitations and for storage units also capacity limits.

$$F = \{(\delta, f_s) \in \mathbb{R}^{n_d+n_s} | C_s f_s + C_d \delta \leq b\} \tag{2.1}$$

5. For explicit determination of feasible combinations of uncertainty, project the flexibility set on the dimensions of the uncertainty. The projection method will be discussed in more detail in section 8.2. Mathematically, the projection can be written as:

$$F_d = \{\delta \in \mathbb{R}^{n_d} | \exists f_s, (\delta, f_s) \in F\} = \{\delta \in \mathbb{R}^{n_d} | G\delta \leq g\} \tag{2.2}$$

   The resulting linear matrix inequality bounds the locational flexibility in terms of feasible δ.

In detailed description of the individual steps are given in [15].

2.3 Illustration

In Fig. 2.1 an illustration of locational flexibility is given. The details on the setup are found in [15]. The flexibility shown is in terms of possible power deviations of three consecutive timesteps. As can be seen, the bounds are depending on the available transmission capacity: while for a grid with large transmission capacity (copperplate) the uncertainty in red can easily be covered, in the case of limited transmission capacity, some realizations of the uncertainty would not be feasible for the given system state.

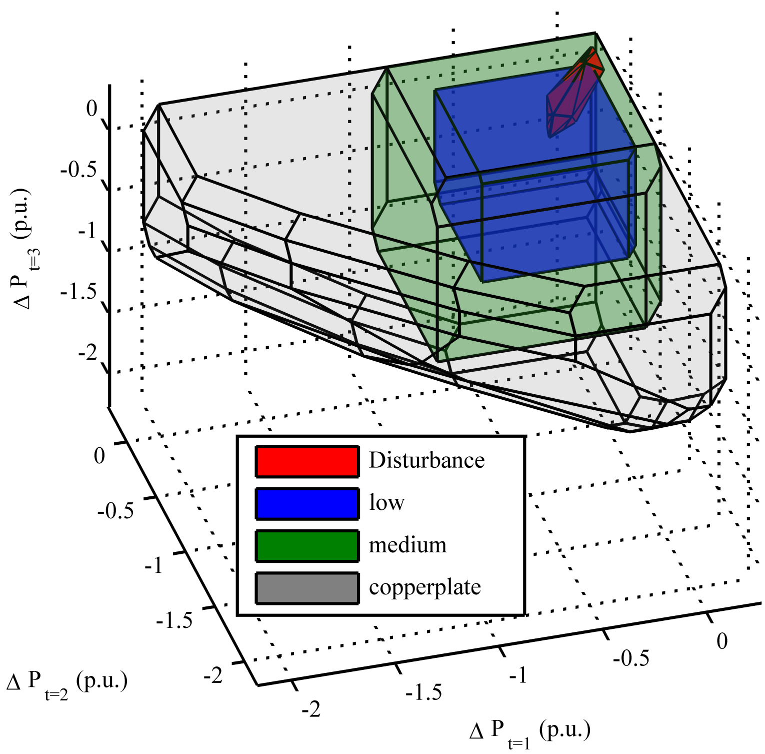

Figure 2.1: Available flexibility at a given bus and comparison with possible local uncertainty for different levels of available transmission capacity.

Chapter 3

Characterization of Uncertainty

3.1 Motivation

The operation of the power system is inherently related with stochasticity both in production and consumption due to partly predictable energy sources and load. Owing to the high shares of fluctuating renewable energy sources (RES), e.g., wind power, system operation is subject to increased *variability*, i.e., random fluctuations of the production driven by the ambient conditions, as well as *uncertainty*, i.e., partial predictability of the actual power output [16]. In turn this uncertainty translates into flexibility needs for the power system which should be taken into account during the stage of reserve procurement. Here we focus on the uncertainty arising from the fluctuating in-feed of RES, but other sources of uncertainty, e.g., load deviations or equipment failures (N-1 security criterion), can be similarly represented.

3.2 Main idea and method

Aiming to express the flexibility needs in a common framework as the locational flexibility, using the $[R,\ P,\ E]$ metric, we construct a polytope of the form $S\delta \leq h$ bounding the disturbances δ based on uncertainty description in form of scenarios. If these scenarios respect the spatio-temporal dependence structure of the prediction errors, e.g., for a number of wind farms in several locations and multiple forecast lead times, the resulting polytope would preserve this information. The complete methodological framework for the generation of spatio-temporal scenarios is provided in [9].

Following an approach similar to [17], the uncertainty set is constructed using a scenario set J. The flexibility metrics for each time interval $[t,\ t+1]$

are calculated as

$$\begin{aligned} R^{t,j} &= (P^{t+1,j} - P^{t,j})/t_s \\ P^{t,j} &= P^{t+1,j} - \hat{P}^t \\ E^{t,j} &= \Big[(P^{t+1,j} - \hat{P}^t) + (P^{t,j} - \hat{P}^t)\Big]\, t_s/2 \end{aligned} \tag{3.1}$$

and a cloud of N_J points is obtained in a space with coordinates R, P and E. The uncertainty set $\mathcal{W}$ is defined as the convex hull (Fig. 3.1) of these points constructed using the Quickhull Algorithm [18].

Since the dispatch of the wind turbine influences the possible deviations, it should be noted that the uncertainty set is constructed based on the expected system state, i.e., $\hat{P}$ is equal to the conditional mean forecast.

3.3 Illustration

Figures 3.1 - 3.2 depict an example of convex hulls obtained using the proposed method for different time intervals of the spatio-temporal scenarios of Fig. 3.1 which represent the uncertainty sets of the stochastic wind power production. In general, higher forecast lead time is expected to increase the volume of the respective uncertainty sets due to the higher uncertainty of the forecasts as shown also by the dispersion of points in the 3 - D space and the wider range of scenarios. However, in time intervals where certain events can be accurately predicted, e.g., between hours 24 and 25 when steep ramping down is expected, the proposed methodology adjusts properly the corresponding dimensions of the convex hull accounting for the low uncertainty.

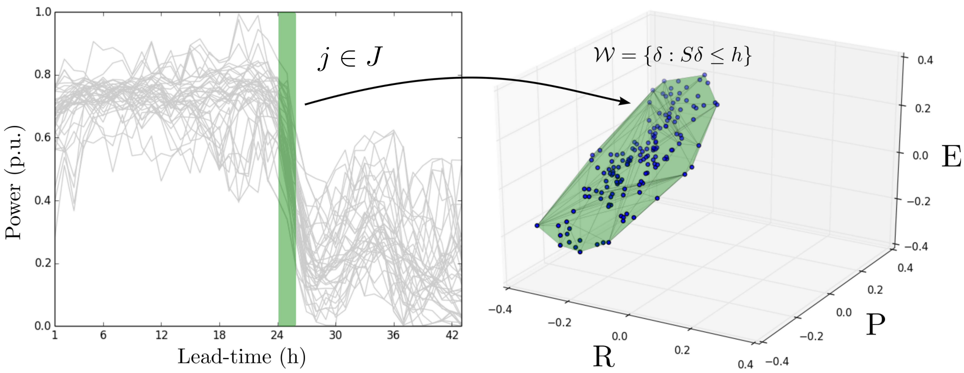

Figure 3.1: From spatio-temporal scenarios to uncertainty set (convex hull) for a period with predicted steep ramping-down event. For illustration, only one time interval (hours 24-25) is displayed.

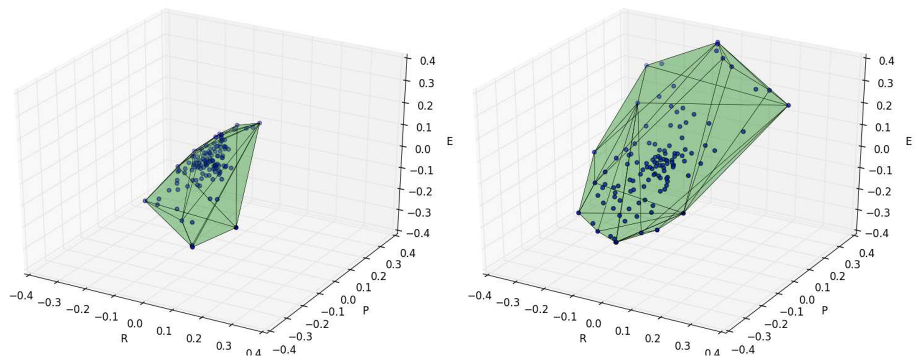

Figure 3.2: Uncertainty sets (convex hull) for time interval 12-13 (low forecast uncertainty) and time interval 36-37 (high forecast uncertainty).

3.4 Potential and limitations

The main advantage of the proposed framework for uncertainty characterization is that allows to capture the spatio-temporal correlations between multiple locations and look-ahead time-steps. This information is of major importance in most of power system operational problems, since aggregated renewables production as well as the system imbalances in real-time are significantly affected by the spatial and temporal characteristics of the environment conditions, e.g., wind and the corresponding prediction errors.

Two main limitations regarding the applicability of this methodology in operational problems can be identified:

1. Availability of high quality forecasts in form of spatio-temporal scenarios. These type of predictions have to be centrally obtained, e.g. by the TSO, and they require a large amount of input information and may involve high computational complexity.

2. The number vertices of the convex hull may increase significantly if a larger amount of wind power locations and time steps is considered. However, this problem can be tackled by applying scenario reduction techniques on the initial scenario set J [19].

Part III

Procurement of Reserves

Introduction to reserve procurement

This part of the report considers the problem of reserve procurement in the presence of uncertainty arising from the variability and the partial predictability of renewables.

The first section employs the formulation of probabilistic power flow taking into account both the forecast errors and the properties of different reserve types, i.e., manual and automatic, as well as the controllability of HVDC interconnections in order to procure the sufficient manual reserves in appropriate grid locations. The second section presents the formulation of an adaptive robust optimization problem that combines the concepts of *locational flexibility* and the uncertainty characterization described in chapter II in order to minimize the total balancing cost, i.e. reserve procurement and activation cost, under the worst-case realization of uncertainty. Finally, the third section studies the effect of transmission capacity allocation for exchange of reserves between neighbouring power system under different market structures that either implicitly optimize this parameter or require to explicitly set it ex-ante.

Chapter 4

Procurement using Probabilistic Power Flow

4.1 Motivation

Traditionally, the N-1 security criterion ensures that the failure of a single component, e.g. a generator outage or a line tripping, doesn't compromise system stability. With increasing shares of intermittent renewable energy sources, the forecast errors adequate consideration. On the one hand, power flows are increasingly uncertain and on the other hand, the often remote location of the renewable energy sources increase the stress on the transmission grid as it was originally built for centralized generation. In this section we explore a formulation of probabilistic power flow that not only incorporates the uncertainties arising from forecast errors but also the influence of manual and automatic control reserves reacting on the uncertainties as well as the properties of new transmission technologies such as HVDC interconnections. The power flow can be used in a procurement algorithm for manual reserves that results in procurement of manual reserve amounts and location such that the risk of congestions is reduced.

4.2 Main idea and method

The probabilistic power flow P_{ac} is formulated as:

$$\begin{aligned} P_{ac} =& S\left(P_g + P_\Delta - P_l + B_{dc}P_{dc} + P_T - d\left(\sum_{i\in n_{bus}} \Delta P_i + P_{T,i}\right)\right) \\ =& S\left(P_g - P_l + B_{dc}P_{dc}\right) + NP_\Delta + NP_T \end{aligned} \tag{4.1}$$

where:

- S: PTDF: Sensitivity of flows w.r.t. power injections [20].
- P_g, P_l: Vector with scheduled power generation and demand.
- B_{dc}: Matrix, mapping the power flows on the HVDC lines P_{dc}, to the corresponding buses in the AC grid.
- P_Δ: Random variable representing uncertainty, e.g. forecast uncertainty, at buses.
- P_T, d: Manually activated reserves and vector which distributes the active power deviation without the deployed manual reserves to automatic control reserve providers.

Formulation (4.1) is also applicable for power systems with multiple control areas. The exact power flow is unknown until the realization of the random variable P_Δ reveals. The uncertain injections result in power flow uncertainties which differ depending on the location. In order to quantify the worst case deviation that can happen on every line, we take the quantile function:

$$dP = F^{-1}_{\Delta P_{ac,l}} \left(\frac{1 \pm \alpha}{2} \right) \tag{4.2}$$

α represents the confidence level and $F^{-1}_{\Delta P_{ac,l}}$ is the inverse cumulative distribution function of the distribution of the power flows on line l. In Fig. 4.1 two extreme cases are shown, where the scheduled power flow is already close to the limit and an overload or N-1 violation would occur in the case of unfavorable uncertainty realizations.

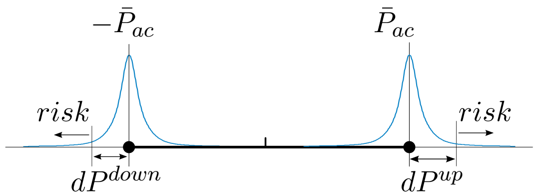

Figure 4.1: Needed upwards and downwards flexibility for a specific transmission line.

This information can be incorporated in various processes, e.g. a combined dispatch and procurement process for manual reserves that considers transmission constraints. One could procure the reserves in different ways, for example:

- Procure reserves and dispatch the generation units so that the scheduled power flows and the worst-case deviations on the power flows are less than the line ratings - also in case of a single outage. This might result in a conservative operation in case of larger uncertainty.

- A second option would be to make use of the location of manual reserves as well as the option of redispatching the flows on HVDC transmission lines when a contingency occurs.

In [21] we demonstrate how the procurement of manual reserves can be done for the second option. The constraint for the inclusion of the flexibility needs in a procurement process happens via power flow constraints of the following form:

$$-\bar{P}_{ac} - dP^{down} \leq S\left(P_g - P_l + B_{dc}P^i_{dc}\right) + NP^i_T \leq \bar{P}_{ac} - dP^{up} \tag{4.3}$$
$$\tag{4.4}$$

where i stands for the scenario considered, e.g. an outage of a generator or a line tripping. In essence, the procurement would make sure to have sufficient capacity of manual reserves in the right locations, but still considering economical aspects. The result would also provide a redispatch policy for the HVDC lines in the case of outages. The detailed formulations are found in [21].

4.3 Illustration

For a simple test case with two wind cases (a lot of intermittent energy sources (high wind case), few intermittent energy sources (low wind case)) the percentage of scenarios resulting in congestions are listed in Tab. 4.1. Two different forecast lead times (3h, 24h) are tested. It can be seen, that reducing the forecast lead time as well as considering the fluctuations results in substantially less congestions. Especially in the high wind case.

Table 4.1: Congestions (%) for 3h and 24h forecast, with/-out risk aversion.

Wind Case Risk Aversion	low -	low $\alpha = .95$	high -	high $\alpha = .95$
3h	0.08	0.06	9.5	4.6
24h	1.5	0.28	13.4	3.4

4.4 Potential and Limitations

The method shows that the placement of flexible units, i.e. reserve providers, as well as flexible transmission devices, such as HVDC, facilitate the integration of intermittent renewable energy sources. The method should be further developed in terms of the modeling of uncertainty, especially correlations, towards an approach considering locationality, automatic and manual reserves and policies on how to operate them.

Chapter 5

Procurement of Locational Flexibility

5.1 Motivation

Considering that the operation of power systems with large scale penetration of renewable energy sources (RES) are significantly effected by the variability of RES production and the forecast uncertainty, TSOs have to incorporate explicit flexibility metrics in their decision-making process and account for the stochastic behavior of the system parameters. Based on the definitions and the mathematical descriptions of locational flexibility and uncertainty sets, an adaptive robust optimization model is formulated to enable their interaction in an operational framework aiming to guarantee the least-cost reserve procurement and activation for the worst-case realization of uncertainty. This advanced reserve procurement method allow the TSO to schedule its balancing operation considering the whole trinity of flexibility and uncertainty characteristics, i.e., ramping, power and energy.

5.2 Main idea and basic equations

The reserve procurement problem is formulated as:

$$\min_{\Delta b, f_s} C_{\mathrm{proc}}^T \Delta b + \mathcal{L}(\Delta b) \tag{5.1}$$

$$\text{s.t. } \Delta b^{\min} \leq \Delta b \leq \Delta b^{\max}, \tag{5.2}$$

where

$$\mathcal{L}(\Delta b) = \max_{\delta} \min_{f_s} C_{\mathrm{op}}^T f_s \tag{5.3}$$

$$\text{s.t. } C_s f_s + C_d \delta \leq b_0 + \Delta b : \mu \tag{5.4}$$

$$\text{s.t. } \delta \in \mathcal{W}. \tag{5.5}$$

This is an adaptive robust optimization problem where the objective function (5.1) to be minimized is the sum of the reserve procurement cost with the cost of the balancing operation under the worst-case realization of the uncertainty $\mathcal{L}(\Delta b_i)$. The first-stage decisions Δb_i, represent the reserve procurement and constraints (5.2) enforce the bounds of the available reserves. The second-stage variables (recourse actions) account for the balancing dispatch f_s, as a response to the realization of the uncertainty δ. The $max-min$ programming problem (5.3)-(5.5) finds the minimum balancing cost for the worst-case realization of the uncertainty. Constraint (5.4) ensures the feasibility of the balancing dispatch for every $\delta \in \mathcal{W}$ given in (5.5). Constraint (5.4) incorporates the flexibility set as in Eq. (2.1).

Considering that the above optimization problem cannot be solved directly given its $min-max-min$ structure, we reformulate the $max-min$ problem using the dual of the right-hand side problem written as:

$$\begin{aligned} \max_{\mu} \ & (C_d\delta - \Delta b - b_0)^T \mu \\ \text{s.t.} \ & -\mu^T C_s \leq C_{\text{op}}^T \\ & \mu \geq 0. \end{aligned} \tag{5.6}$$

Hence, we obtain the following $min - max$ optimization problem, where we have merged the two maximization problems into a single maximization problem with decision variables δ and μ.

$$\begin{aligned} \min_{\Delta b} \ C_{\text{proc}}^T \Delta b + & \max_{\delta,\mu} \ (C_d\delta)^T \mu - (\Delta b + b_0)^T \mu \\ & \text{s.t.} \ -\mu^T C_s \leq C_{\text{op}}^T \\ & \qquad \mu \geq 0 \\ & \qquad \delta \in \mathcal{W} \\ \text{s.t.} \ \Delta b^{\min} \leq \Delta b \leq \Delta b^{\max}. & \end{aligned} \tag{5.7}$$

It should be noted that the objective function (5.7) includes a cross-product of the variables δ and μ and thus the resulting optimization problem is bilinear. If the uncertainty set $\mathcal{W}$ is a polyhedral set, then the optimal solution will be one the vertices of this set. In addition, since the first-stage variables Δb_i do not appear in the constraints of the bilinear problem, the feasible polyhedron has a finite number of vertices $v = A, ..., H$ (in other words the feasible polyhedron in independent of the 1st stage decisions).

Finally, the our model can be further reformulated introducing the auxiliary variable C_{op}^{wc} representing the worst-case resource cost $\mathcal{L}(\Delta b_i)$, equal to the optimal objective function of the $max - min$ problem (5.3)-(5.5).

$$
\begin{aligned}
\min_{\Xi} \quad & C_{\text{proc}}^{T}\Delta b + C_{\text{op}}^{\text{wc}} \\
\text{s.t.} \quad & C_{\text{op}}^{\text{wc}} \geq C_{\text{op}}^{T} f_{s,\nu}, && \forall \nu = A, ..., H \\
& C_s f_{s,\nu} + C_d \delta_\nu \leq b_0 + \Delta b, && \forall \nu = A, ..., H \\
& \Delta b^{\min} \leq \Delta b \leq \Delta b^{\max},
\end{aligned}
\tag{5.8}
$$

5.3 Illustration

To illustrate the applicability of the proposed method in system planning and scheduling operations, we consider two possibilities to add flexibility to the system operation, namely: *i.* curtailment of intermittent energy sources and *ii.* units with storage capacities (e.g. pumped hydro storage) and we vary the amount of wind energy that can be curtailed (in percent of actual production) as well as the storage capacity available [15].

In Fig. 5.1 the capacity costs for the procured reserves as a function of the share that can be curtailed and the size of the storage at bus 1 are shown. The storage is charged to 50% of the capacity. The reserves are procured according to (5.8) for a given uncertainty set and the costs are calculated as $C_{\text{proc}}^{T}\Delta b$. It can be observed that the cost decrease in the given system for increasing storage sizes as well as the possibility to curtail intermittent infeeds. The least costs are achieved by a suitable combination of both remedies.

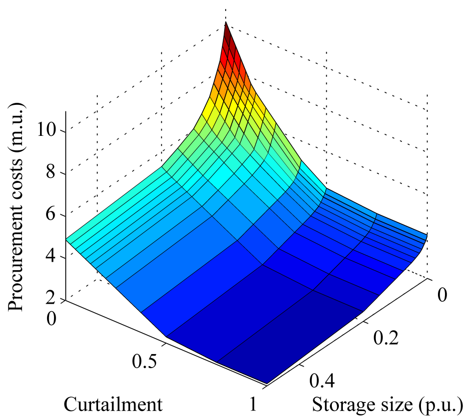

Figure 5.1: Capacity reservation costs as a function of curtailment and storage size.

5.4 Potential and Limitations

The method for procurement of locational flexibility, in terms of control reserves, guarantees the ability of the power system to contain the worst-case realization of uncertainty with the lowest possible cost. This method can be readily applied by TSOs given the availability of uncertainty information in form of a polyhedral set. Nonetheless, it should be noted that the solution of model (5.8) requires the enumeration of all the vertices ν of the uncertainty set $\mathcal{W}$, which may result in intractable problems if the number of vertices becomes very large. However, the structure of this problem allows to employ more efficient solution schemes, e.g., based on Benders Decomposition [22]. In this case, the optimal solution of the procurement problem can be obtained iteratively, adding a Benders cut for each vertex of the uncertainty set until the convergence criterion is met.

Chapter 6

Transmission Capacity Allocation for Cross-border Exchange of Reserves

6.1 Motivation

The European power system is undergoing significant restructuring both in terms of generation capabilities and market architecture. Given the current European market setup, where reserve capacity, forward and balancing market-clearings are performed sequentially, the ex-ante allocation of transmission capacity between these trading floors is necessary. However, this procedure is subject to uncertainty due to the significant time interval between day-ahead scheduling and actual operation. The two main approaches to cope with this uncertainty are stochastic programming and deterministic models. Despite the theoretical advances of the former, current operational practices are based on deterministic and usually static reserve requirements. For instance, in the new HVDC interconnection between Denmark and Norway (Skagerrak 4), 15% of its capacity will be permanently reserved for exchange of ancillary services [23].

6.2 Main idea and method

Three alternative market-clearing models are employed to settle the *reserve capacity*, *day-ahead* and *balancing* markets, described as:

1. Stochastic energy and reserve co-optimization
2. Deterministic market-clearing
    - (a) Energy and reserve capacity co-optimization
    - (b) Sequential clearing of reserve capacity and energy markets

All the market setups considered in the present work are based on the following assumptions:

1. only wind power uncertainty is considered assuming that load and availability of conventional generators are perfectly known,

2. demand is completely inelastic and

3. the market settles on an hourly basis and each trading period is independent since no inter-temporal constraints, e.g., ramping limits, are considered.

The stochastic energy and reserve co-optimization market model determines the the optimal amount of reserves and the day-ahead dispatch taking into account the anticipated real-time operation of the power system, through a finite set of scenarios that captures the spatial dependence structure of the forecast errors. This formulation performs an intrinsic trade-off between the value of the available resources in the day-ahead (energy and reserve capacity) and the balancing (reserve deployment) stages, while it enables an implicit allocation of the transmission capacity among energy and reserve services.

In order to avoid the computational burden of the stochastic market-clearing approach, market operators employ deterministic models which have to procure reserve capacity based on explicit reserve requirements in order to deal with unforeseen events during real-time operation. The deterministic energy and reserve capacity co-optimization models allows for simultaneous procurement of energy and reserves while the sequential clearing of these trading floors decouples completely these two services through an independent settlement of the energy and reserve capacity markets. Both market organizations include a real-time balancing mechanism to compensate any deviations from the day-ahead schedule.

The first market setup finds the optimal day-ahead dispatch and yields an implicit optimal transmission capacity allocation between energy and reserves, based on a single-valued forecast (conditional expectation) of wind power production, taking into account the explicit system-wide reserve requirements. On the other hand, the second market architecture requires the explicit allocation of transmission capacity for reserve exchange as well as the definition of reserve requirements for each area of the power system. Any corrective actions during real-time operation are compensated through a balancing market considering that a single pool of control resources is accessible from all areas.

The market-clearing models discussed above are described in detail (complete mathematical formulation of the optimization models) in [24]. In addition, [24] outlines a methodology for the determination of reserve requirements and the modeling of wind power uncertainty in the context of this study.

6.3 Illustration

The performance of the market-clearing algorithms described above is evaluated on a two-area power system. Analytic results and further details on the case study data presented in [24]).

As an illustrative example studying the effect of the explicit transmission allocation X on the expected system cost, we consider a reserve market where OCGT, IGCC and CCGT units provide 50%, 40% and 40% of their capacity for reserve provision at a price equal to 15%, 30% and 30% of their day-ahead offer, respectively. For a constant wind penetration level of 24%, we perform a 'grid-search' on the HVDC tie-line capacity and the parameter X, to obtain the corresponding expected system cost displayed in figure **??**. The shape of this surface allows to identify three main directions aiming to analyse the effect of these parameters on the overall market efficiency. Note that the dotted line $\mathcal{L}$ represents the locus of the least-cost points for different HVDC capacities. Moving along direction A on the left-hand side of $\mathcal{L}$, the expected cost reduces as the tie-line capacity increases since a larger pool of common resources is accessible from both areas. A similar trend applies for larger values of X (direction B), where the reserve capacity market does not alter significantly the optimal day-ahead settlement by imposing additional constraints. For example, in a segmented market of reserve resources (low X), expensive units may be assigned to provide downward reserve, enforcing a corresponding lower bound on the energy dispatch, out of the merit order. Large values of X on high HVDC capacity (direction C), allow the reserve market to pick more economical resources based solely on their capacity payment. However, this translates into increased expected balancing cost if mainly excess production situations occur during actual operation, i.e., generators with low marginal (and reserve capacity) cost are willing to buy back their production in lower price.

6.4 Potential and Limitations

The mathematical framework described in this work allows to study and evaluate the efficiency of different market-clearing models on the settlement of reserve capacity, day-ahead and real-time (balancing) markets. Setting as benchmark the stochastic energy and reserves co-optimization, one can

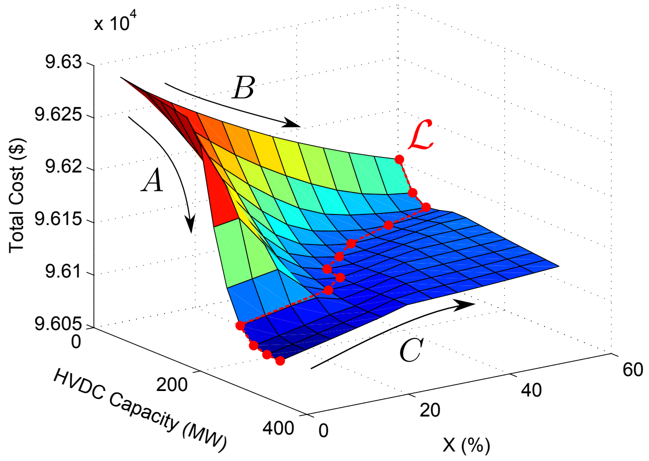

Figure 6.1: Impact of HVDC capacity and transmission allocation X on the expected cost of sequential market-clearing.

analyse the efficiency of different deterministic market designs to accommodate large shares of wind power and assess the gain arising moving towards tighter coordination between different trading floors. Despite that the relative difference in market efficiencies may be highly sensitive to the system properties and the market dynamics, there generally exists an optimal allocation to be made, which however may dynamically vary depending on generation, load and system uncertainties.

Future work may focus on the reformulation of the deterministic energy and reserve co-optimization algorithm by defining per area reserve requirements in order to reveal the optimal transmission capacity allocation of this model. This could serve as an insight towards an explicit rule that determines the optimal percentage of the tie-line capacity to be designated to reserve exchange in the sequential design. Further extensions could investigate the issues related to HVDC and AC network coordination as well as integrate the aspect of cross-border reserve provision in the HVDC expansion planning.

Part IV

Activation and Coordination of Reserves

Introduction to reserve activation and coordination

In this part, we explore alternative operational strategies during the balancing stage as well as the necessary information exchange between neighbouring TSOs in order to enable coordination of their decisions during real-time operation.

The first section of this chapter, describes a framework to define the main components of predictive operational strategies and evaluate the most crucial properties in a systematic way based on several criteria. The second section proposes a method to communicate available flexibility expressed in terms of possible tie-line flow changes. This method allows the TSOs to share only the necessary information with the neighbouring systems, without disclosing the full details of their internal network state.

Chapter 7

Predictive Dispatch of Control Reserves

7.1 Motivation

The current European market design is based on the sequential clearing of the day-ahead, intra-day and balancing markets and it is suitable for electricity generation based on conventional power plants, where operation schedules need to be coordinated and planned ahead and reserve needs are driven by the outages of generation units or transmission lines. In this conventional operation paradigm system balancing is mainly reactive, and reserve needs are static.

In power systems with high shares of intermittent RES, generation becomes strongly fluctuating and only partly predictable, so that conditions for the conventional operation paradigm are no longer satisfied. In order to improve economy and availability of balancing resources, the activation of control reserves can be altered from reactive and restorative to predictive dispatch using forecasts with smaller prediction errors. This work considers predictive dispatch strategies for intra-hour balancing investigating alternate optimality criteria and product constraints.

7.2 Main idea and method

The predictive dispatch of regulating power can be based either on deterministic or on stochastic forecasts of the power imbalances during the real-time operation.

Deterministic Dispatch

The deterministic dispatch model finds the optimal schedule $P^{M,*}$ of manual reserves that minimizes the objective function $J^M(P^M)$ as:

$$\underset{P^M}{min} \quad J^M(P^M) \tag{7.1}$$

subject to

$$h^M(P^M, \hat{P}^{imb}) = 0 \tag{7.2}$$
$$g^M(P^M, \hat{P}^{imb}) \leq 0 \tag{7.3}$$

where $\hat{P}^{imb}$ is the vector of expected system imbalances. The equality constraints (7.2) include the system balance constraints and the decomposition of the energy supply curve into blocks. Constraint (7.3) specifies the operational limits of the power system as well as the dispatch limits of the regulating power bids. Given the vector P^{imb} of the actual imbalances, the automatic reserve dispatch P^A is the vector that satisfies the real-time power balance and operational constraints:

$$h^A(P^A, P^{imb}, P^{M,*}) = 0 \tag{7.4}$$
$$g^A(P^A, P^{imb}, P^{M,*}) \leq 0 \tag{7.5}$$

Constraint (7.4) requires that the remaining imbalance $P^{imb} - P^{M,*}$ will be covered by the automatic response, while constraint (7.5) ensures that this response respects the operational and reserve limits.

Stochastic Dispatch

The accurate representation of the uncertainty requires the consideration of the interdependence structure of the prediction errors. In the operational strategies, this stochasticity is represented using a set S of scenarios spanning the full range of plausible realizations of the stochastic imbalance $\mathcal{P}^{imb}_{t+k}$. Each scenario $s \in S$ is characterized by a vector of imbalances P^{imb}_s, which respects the temporal interdependence structure of the prediction errors.

Operational strategies are modeled as a two-stage stochastic programming problem, where the first stage ($st1$) decisions represent the activation of manual control reserves and the second stage ($st2$) represents the activation of automatic reserves at every given scenario. The stochastic dispatch model is described by the following optimization problem:

$$\underset{P^M, P^A}{min} \quad J^{M,st1}(P^M) + \mathbb{E}_s[J^{M,st2}_s(P^A_s)] \tag{7.6}$$

subject to

$$h_s(P^M, P_s^A, P_s^{imb}) = 0 \quad \forall s \tag{7.7}$$
$$g_s(P^M, P_s^A, P_s^{imb}) \leq 0 \quad \forall s \tag{7.8}$$

where $\mathbb{E}_s[\cdot]$ is the expectation operator over the scenario set S. Constraints (7.7) and (7.8) are equivalent to (7.2) and (7.3) for every scenario $s \in S$.

Definition of Operational Strategies

The definition of operational strategies is essential because they provide the necessary link between the available balancing power products and the decision-making policy of the TSO, as illustrated in Fig. 7.1. The main components of an operational strategy are:

1. The TSO Policy.
   (a) The objective function J^M.
   (b) The grid constraints h^O and g^O.
   (c) The operation timing T^O.
2. The reserve product definition
   (a) Market timing T^P.
   (b) Product constraints h^P and g^P.

7.3 Illustration

The method is exemplarily applied to a case study in order to illustrate the formulation of different operational strategies and assess their performance based on several criteria, such as: *i.* total operating cost, *ii.* energy utilization and *iii.* maximum power capacity of manual and automatic reserves. The complete description of the test case power system, wind power uncertainty characterization and the underlying assumptions are described in [25].

Figure 7.2 provides an illustration of the actual dispatch of automatic and manual reserves for an operational strategy with minimum up time $T_{min}^{up} = 60min$ and lead-time $T^{lt} = 15min$ which aims to minimize the expected balancing cost. The reserve activation of different operational strategies follows a similar pattern, which is mainly dictated by the sign and the magnitude of the forecast imbalance. However, the exact amount of each reserve type activated in every period changes depending on the applied operational strategy.

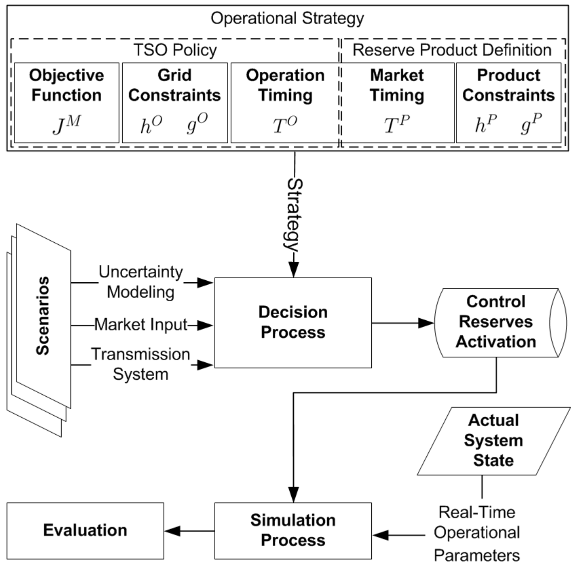

Figure 7.1: Illustration of operational strategies concept for control reserves activation.

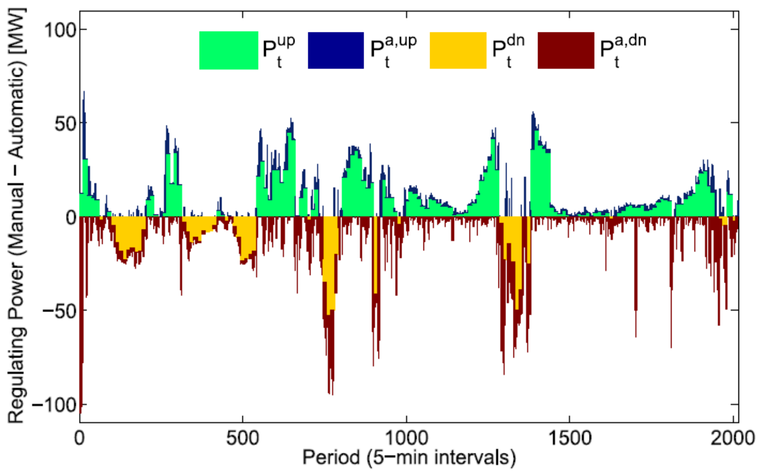

Figure 7.2: Dispatch of manual and automatic reserves for operational strategy with parameters $T^{up}_{min} = 60$ min, $T^{lt} = 15$ min, Objective: cost minimization

7.4 Potential and limitations

This work provides a framework for the definition and formulation of operational strategies for reserve activation focusing on the predictive dispatch of regulating power needed to cope with wind uncertainty. Alternative operational strategies in terms of product specification, timing and availability of balancing resources are formulated and evaluated using performance criteria. The results of the case study have shown that variations in performance indices can be significant and these trade-offs should be considered during the decision-making process. The most significant impact on the performance metrics arises from variations in the balancing products definition, which highlights also the importance of power system flexibility.

The proposed dispatch strategies are based on a stochastic programming formulation which requires the accurate representation of uncertainty in form of scenarios that capture the temporal dependence structure of the forecast errors. In case the TSO wants to include also any network representation, e.g., transmission capacity constraints, into its decision-making process, these scenarios should also be able to capture the spatial correlation between multiple wind locations. The current framework can be further upgraded including energy and ramping constraints, as these limits become highly significant in power systems with high shares of variable renewable energy sources.

Chapter 8

Inter-TSO coordination of Flexibility

8.1 Motivation

With increasing planning and forecast uncertainty, limited transmission capacity availability as well as reduced availability of conventional controllable generation units for balancing, methods are needed to improve the coordination of flexibility between different TSOs.

8.2 Main idea and method

For an efficient coordination, we determine bounds on the possible tie-line flow changes as a way of communicating the available flexibility. These bounds, based on a current system state, can be exchanged with neighboring TSOs and would be integrated in their operation procedures, e.g. in re-dispatch or balancing operation. These bounds, given by linear matrix inequalities, can incorporate manual reserves and transmission constraints, but they are constructed such that possibly sensitive information is not reconstructable.
In Fig. 8.1 the abstraction of a power system that consists of two independently operated areas is shown. This power system is further modeled as system with multiple inputs and multiple outputs (MIMO system) as in Fig. 8.2.

For a single area, the operational constraints, including power balance, transmission limits, available reserves, ramping constraints and N-1 security constraints, are written in form of Eq. (8.1). For a given system dispatch, the internal deviations p_i, i.e. the activation of manual reserves, are related to changes of the tie-line flows p_e. If no flexibility is available to share with neighboring TSOs, p_i is set to zero. In this case, the equation becomes

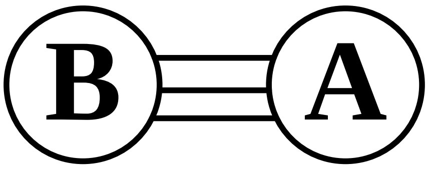

Figure 8.1: Two area system.

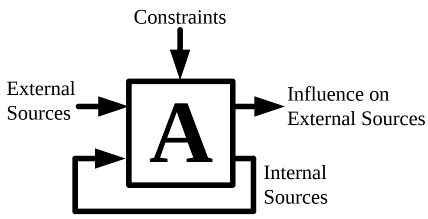

Figure 8.2: MIMO System.

comparable to an ATC (available transmission capacity) value.

$$F = \{ (p_i, p_e) \in \mathbb{R}^{n_i} \times \mathbb{R}^{n_e} | C_i p_i + C_e p_e \leq b\} \tag{8.1}$$

In order to reduce the data in F, to protect confidential data as well as to get an explicit bound on the tie-line changes for the neighboring TSO (i.e. the local TSO wants to decide with resources he offers to his neighbor), we use a projection of the polytope F on the relevant dimensions, in our case the tie-line flow deviations. This concept is illustrated in Fig. 8.3 for a single generator that provides reserves and two tie-lines.

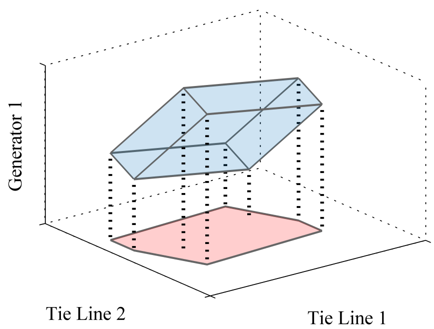

Figure 8.3: The projection represents the feasible set for the external sources.

Mathematically, this can be written as Eq. (8.2):

$$F_e = \{p_e \in \mathbb{R}^{n_e} | \; \exists \; p_i, (p_i, p_e) \in F\} = \{p_e \in \mathbb{R}^{n_e} | \; G p_e \leq g\} \tag{8.2}$$

The resulting polytope F_e, which every TSO generates for his area, are exchanged bilaterally between TSOs on a regular basis. The information about available flexibility from neighboring systems can directly be integrated, e.g. in a re-dispatch optimization. The method is described in detail [26]. Extensions to express the redispatching costs were presented in [27] and an application in multi-terminal HVDC grids is sketched in [28].

8.3 Illustration

The method is exemplarily applied to the IEEE RTS-96 system consisting of 2 zones that are interconnected with three tie-lines. In Fig. 8.4 the allowed deviations away from the scheduled power flows on the tie-lines are shown.

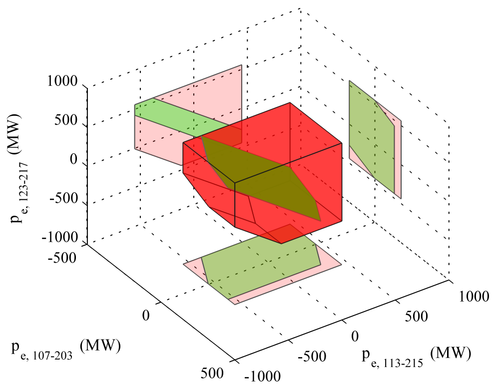

Figure 8.4: Feasible tie-line flow deviations in IEEE RTS-96 2 zones test system.

8.4 Potential and limitations

The case studies show the potential of the framework. Main observations indicate that the tie-line utilization can be improved compared to the balancing operation with prevalent ATC calculation methods. This allows to balance larger deviations e.g. due to forecast errors of renewable energy sources. Further, it provides TSOs a tool to determine and assess possible re-dispatch or balancing operations respecting transmission constraints in the local and neighboring areas. The framework is easily extendable: the method can be applied to more than two areas using an iterative algorithm, the lower bound for redispatching costs a neighboring TSO would face can be approximated using a cutting-plane method and finally, future research could identify market products to trade this *exportable flexibility*.
The major limitation are the computational complexity for the projection and the need for substantial amount of data. The reduction of the computational complexity should be the focus of future research.

Part V

Grid Expansion considering Operational Flexibility

Introduction to grid expansion considering operational flexibility

In this part, we illustrate for a few selected examples how the operational flexibility of a power system can be extended using new technologies or how flexibility can be considered in existing tools for expansion planning. The first two sections are dedicated to dynamic line ratings, i.e. methods that allow to increase the transmission capacity under suitable meteorological conditions. The next section discusses how flexibility can explicitly be considered in grid expansion algorithms. Finally, we discuss two modeling approaches for technologies that allow a more flexible operation system in a $C0_2$-neutral way.

Chapter 9

Control-based Grid Expansion using Dynamic Line Ratings

9.1 Motivation

The thermal limits of transmission lines are selected based on conservative assumptions on prevalent meteorological conditions, such as high ambient temperatures and low wind speeds. However, during most periods the meteorological conditions allow for more current being transmitted without overheating the lines. Further, the conductors have a certain thermal inertia and thus the lines could also be overloaded for a limited time amount. In the context of this report, we consider *Dynamic Line Rating (DLR)* as the possibility of the system operator to adapt the line ratings for a steady-state operation based on current meteorological conditions or their forecasts. Further information about the potential, modeling and further literature can be found in [29], [30].

9.2 Main idea and method

In the scope of the project, two ways to enable DLR were developed. Each method is briefly introduced in the next paragraphs.

9.2.1 N-1 security assessment incorporating dynamic line ratings

The first method combines a dispatch optimization which incorporates the well-known N-1 security criterion together with DLR. As the dispatch planning is done with a reasonable time delay to the realtime operation, e.g. day-ahead, the meteorological conditions are given only as a forecast with empirical distributions of their forecast errors and thus the ampacity of the conductors are given as a random variable depending on the weather forecasts. In a standard security-constrained economic dispatch or unit commitment, the transmission limits are thus not given by a fixed value anymore but rather the optimization needs to determine a unit commitment/dispatch that satisfies the risk aversion of the operator. The main equation of the dispatch can be written as:

$$\min_{P_G} \; f\left(P_G\right) \text{ subject to } g\left(P_G\right) = 0 \tag{9.1}$$

Problem (9.1) minimizes costs associated with the operation of generation units P_G subject to constraints. The constraints contain for example limits of the generators, account for deviations using spinning reserves and ensure an active power balance. For the transmission limits a so-called *chance constraint*, i.e. a constraint that needs to be satisfied with a given probability, is needed.

$$\mathbb{P}\left(\delta \in \mathbb{R}^{N_s N_m} \;\middle|\; \begin{array}{l} \left|K^i P^i\right| \leq P^i_{\text{DLR}}\left(\delta\right) \\ \text{for } i = 0, \ldots, N_{\text{out}} \end{array} \right) \geq 1 - \epsilon \tag{9.2}$$

$P^i_{\text{DLR}}\left(\delta\right)$ is a vector with all the line ratings which are a function of the distributions of the weather conditions δ. The constraint has to be satisfied with probability $1 - \epsilon$ for all N_{out} possible line outages and the normal operating condition. The power flows are determined by linearized power flow equations, i.e. K^i is a sensitivity matrix that maps net bus injections P^i to corresponding line flows.

A scenario based methodology is applied to solve the above chance-constrained problem. The scenarios are created using a copula approach which captures the relations between forecasts and actual realization of different meteorological conditions. More details are found in [29].

9.2.2 Robust Corrective Control Measures in Power Systems with Dynamic Line Rating

The second approach uses corrective control actions instead of a chance-constraint as in the first approach. The corrective control actions are enabled in case of an imminent line overloading. Using robust optimization approaches, sufficient capacity from flexible resources in suitable locations of the grid are procured. This results in additional transmission capacity that can be used but is still protected against overloads by suitable remedial actions. The corresponding constraint in the robust optimization problem takes the form:

$$\begin{aligned} &\left|P_L + f\left(\Delta, \delta\right)\right| \leq \delta \;\forall \delta \in \mathcal{W} \\ &\Delta \in \mathcal{R} \end{aligned} \tag{9.3}$$

where P_L is the scheduled power flows and $f(\Delta, \delta)$ is a function describing corrective control actions that depend on the realization of the uncertain ampacity δ which can take values given by the uncertainty set $\mathcal{W}$.
We present two procurement algorithms with different assumptions on the recourse function f:

- f is an affine policy of the uncertainty, i.e. the realization of the uncertain variable δ linearly maps to changes of certain generation outputs, similar to spinning reserves that are operated pro-rata. The mapping matrix is a result of the procurement. This approach can be operated in a decentralized manner.

- The second algorithm doesn't assume any structure for f but tests all the extreme scenarios of $\mathcal{W}$. The output of f is then the result of an optimization that is calculated once the realization of δ has become known. This approach needs centralized coordination.

More details are found in [30].

9.3 Illustration

9.3.1 Approach I (Chance-constrained Dispatch)

In Fig. 9.1 we exemplarily demonstrate the effect of different security levels by varying ϵ and for different weather forecast lead times ranging from 24h (red) over 12h (orange) to 3h (green) on the feasible scaling factor, with which we scale the total demand uniformly. In turquoise the scaling factor for perfect forecast knowledge is shown. There are two observations: first, a reduction in the forecast lead time increases the grid utilization and second, increasing security levels decrease the utilization.

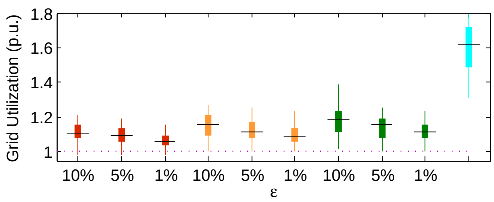

Figure 9.1: Scaling factors for Demand for different forecast lead times and different security levels.

9.3.2 Approach II (Corrective Control Measures)

The approach is illustrated in Fig. 9.2. In red the joint distribution function of the line ratings of two transmission lines is shown. The cuts represent exemplarily selected line ratings. The green circle bounds the 95% quantile of the distribution. It is observed that for the given selection of line rating 1 there exists a certain risk of line overloading. The methods procure sufficient flexibility for cases where the line rating would effectively be lower than the nominal line rating. Traditionally, the ratings would be chosen more conservatively and thus given up a large potential of transmission capacity.

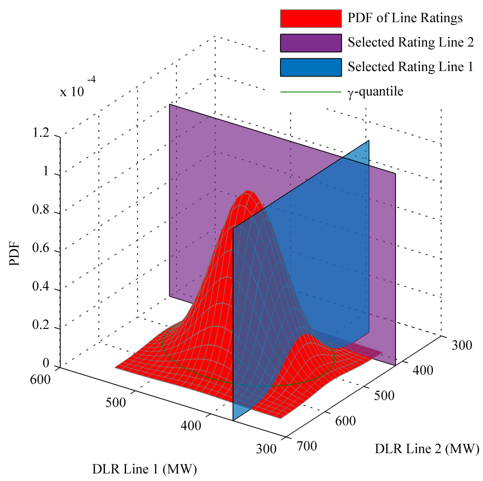

Figure 9.2: Illustration of uncertainty in line ratings and selection of nominal line rating.

9.4 Potential and limitations

The methods demonstrate two basic approaches on how to integrate DLR in operation processes. However, there are still major issues and open questions, some of them are briefly listed next:

- Monitoring: Where to place monitoring equipment? How to integrate the measurements in operation processes?
- Monitoring: How to identify the most critical segments along a transmission line?
- Monitoring: Resilience against communication failure?
- How to integrate DLR in a market environment?
- Dynamic behaviour: How to properly account for the transient behaviour and line aging in temporary overloaded cases?

- Identification of other constraining factors, such as transformer limitations.

Chapter 10

HVDC Grid Expansion considering Flexibility

10.1 Motivation

The increasing shares of fluctuating renewable energy sources, such as wind or solar power, as well as the efforts toward a common European energy market have a major influence on the power transmission. On one hand, the power is transmitted over longer distances and on the other hand, the power flow patterns are changing more frequently. With the more frequent unscheduled changes in the power output and the reduced availability of fully controllable units, such as hydro power units and gas turbines, reserve operation schemes need to be reconsidered. Usually flexibility, i.e. the ability of the system to react on a deviation in power injection, is provided by controllable fast-ramping units, such as storage hydro power plants or gas-fired power plants. Due to limited transmission capacities the flexibility can be dependent on the location in the grid. One of the predominant options to improve the transmission capabilities, is the construction of an overlay grid using multi-terminal HVDC interconnections. Different approaches for grid expansion with HVDC have been proposed. We presented an optimization-based methodology that finds optimal placements of the terminals of the HVDC overlay grid. Compared to other algorithms the placement algorithms optimizes not only economical aspects but also considers the flexibility that is added due to the controllable HVDC grid and can be used for balancing or ramping operation.

10.2 Main idea and method

The system's operational flexibility can be increased if the terminals in a multi-terminal are placed accordingly. HVDC lines inherently don't have generation capabilities, but the flexibility is added due to the controllability of the power flows on the HVDC lines, which often span often long distances and thus can efficiently transfer big amounts of energy, e.g. such that congestions in the underlying AC-grid are reduced.

The method determines the available operational flexibility by considering a *virtual unit* at every bus of the system and maximizing the additional power that can be injected or consumed based on a given system state. The flexibility is determined for every bus, for different system scenarios, e.g. demand scenarios, and for different time periods (e.g. 5min, 15min, 1h, ...). The reason to include the latter one is to account for ramping constraints of generation units that might be imposed. As the flexibility needs might be different at different locations in the grid, the flexibility at a certain bus should only be considered in an optimization if the flexibility requirements are not yet met, e.g. a bus where a wind farm is attached. The flexibility requirements are defined based on different factors, such as the short-term load forecast error, generation forecast errors, e.g. wind and solar or generation outages.

The optimization then places HVDC interconnections in an overlay grid and finds a trade-off between the economical benefits of reduced operational costs and reduced total lack of flexibility at different buses. The objective function is given as:

$$\min \rho \cdot \Upsilon + (1 - \rho) \cdot \Theta \quad \rho \in [0, 1] \tag{10.1}$$

Υ represents the cumulative, normalized lack of flexibility and Θ accounts for the total, normalized operational costs of the system. ρ is a tuning parameter for the system planner which reflects his preference towards reduced costs or increased flexibility. The optimization problem is subject to different constraints, such as:

- constraints related to HVDC, e.g. capacity limits, placement options and enforcement of multi-terminal topology,
- constraints related to the underlying AC grid,
- different generation dispatch scenarios,
- operational constraints of generators providing reserves, e.g. ramping or capacity limits,
- active power balance.

The model can incorporate different scenarios for demand, uncertainty requirements, generator or transmission line availability etc. The detailed method is found in [31].

10.3 Illustration

For an example grid ([31]), the placements are determined for different values of ρ and different number of lines added. In Fig. 10.1 the operational costs are shown. We can see, that for an increasing ρ the operational costs increase, but also the available flexibility in the system (not shown here, cf. [2]) increases. Adding more than one HVDC line results reduces the operational costs even further. With one exception, the costs are smaller compared to the system operation without additional HVDC lines. It should be noted, that the investment costs are not considered in the optimization but only operational costs and flexibility are traded-off against each other.

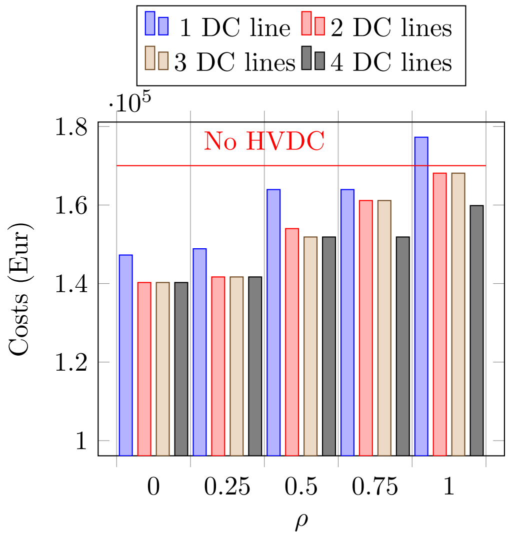

Figure 10.1: Operational costs for different values of ρ and different numbers of HVDC lines.

10.4 Potential and limitations

The method contributes in the HVDC placement problem by considering the flexibility as well. Future research should extend on different aspects. A few examples are given: The investment costs are not considered, which depend on the locations selected. These costs should be reflected properly as well as the feasible connections given by geographical factors. The determination of the flexibility could be improved, i.e. the disturbances in general occur not in a single location but might be correlated over different buses, e.g. forecast errors of wind power injections. Lastly, the computational complexity should be addressed if the algorithm has to be run on large systems with many different flexibility providers, different scenarios and numerous placement options. However, in placement problems the time is usually not critical.

Chapter 11

Conclusion

This report listed, described and exemplarily applied the tools and methods that have been developed within the scope of the BPES project. The methods are grouped into five different categories:

- wind forecasting: presenting a method to produce high-quality wind power forecasts in form of scenarios that can be used in operational tools such as stochastic unit commitment,
- characterization of operational flexibility: a method to describe the operational flexibility and its combination with a compatible description of forecast uncertainty respecting their location in the grid,
- procurement of reserves, where first a probabilistic power flow is presented that considers the influence of reserve operation, then a method to procure reserves respecting locational flexibility needs is given and finally, a third method looks into the allocation of cross-border capacity to exchange reserves with neighboring control areas,
- activation and coordination of reserves, where first a method for predictive dispatch of control reserves is presented and then a method to manage the flexibility between different control areas is shown,
- and the last category focuses on methods to increase the operational flexibility by grid expansion. Two methods present a control-based grid expansion, i.e. an increase of capacity of the lines by means of control-based method, in our case the integration of dynamic line rating, and the last method presents an expansion tool for HVDC grids, that considers the change in flexibility of the transmission system.

Every method is briefly motivated, sketched, exemplarily applied and illustrated as well as their potential and limitations are discussed. The detailed formulations given by referenced publications. In the report on work package 5 [2], the methods are applied to larger case studies demonstrating their effect and performance with respect to different challenges that system operators are currently facing.

Bibliography

[1] M. Bucher, S. Delikaraoglou, K. Heussen, G. Andersson, "BPES Project - Report on Modelling and Characterization," https://www.eeh.ee.ethz.ch, Tech. Rep., 2014.

[2] ——, "BPES Project - Report on Case Studies and Verification," https://www.eeh.ee.ethz.ch, Tech. Rep., 2015.

[3] G. Giebel, R. Brownsword, G. Kariniotakis, M. Denhard, and C. Draxl, "The state-of-the-art in short-term prediction of wind power: A literature overview," ANEMOS. plus, Tech. Rep., 2011.

[4] Y. Zhang, J. Wang, and X. Wang, "Review on probabilistic forecasting of wind power generation," *Renewable and Sustainable Energy Reviews*, vol. 32, pp. 255–270, 2014.

[5] P. Pinson, "Wind energy: Forecasting challenges for its operational management," *Statistical Science*, vol. 28, no. 4, pp. 564–585, 2013.

[6] G. Papaefthymiou and P. Pinson, "Modeling of spatial dependence in wind power forecast uncertainty," in *Probabilistic Methods Applied to Power Systems, 2008. PMAPS'08. Proceedings of the 10th International Conference on.* IEEE, 2008, pp. 1–9.

[7] P. Pinson, H. Madsen, H. A. Nielsen, G. Papaefthymiou, and B. Klöckl, "From probabilistic forecasts to statistical scenarios of short-term wind power production," *Wind energy*, vol. 12, no. 1, pp. 51–62, 2009.

[8] A. J. Smola and B. Schölkopf, "A tutorial on support vector regression," *Statistics and computing*, vol. 14, no. 3, pp. 199–222, 2004.

[9] S. Delikaraoglou and P. Pinson, "High-quality wind power scenario forecasts for decision-making under uncertainty in power systems," in *13th International Workshop on Large-Scale Integration of Wind Power and Transmission Networks*, 2014.

[10] R. Koenker, *Quantile regression.* Cambridge university press, 2005.

[11] P. Kundur, J. Paserba, V. Ajjarapu, G. Andersson, A. Bose, C. Canizares, N. Hatziargyriou, D. Hill, A. Stankovic, C. Taylor *et al.*, "Definition and classification of power system stability ieee/cigre joint task force on stability terms and definitions," *Power Systems, IEEE Transactions on*, vol. 19, no. 3, pp. 1387–1401, 2004.

[12] Y. Makarov, C. Loutan, J. Ma, and P. de Mello, "Operational impacts of wind generation on california power systems," *Power Systems, IEEE Transactions on*, vol. 24, no. 2, pp. 1039–1050, 2009.

[13] A. Ulbig and G. Andersson, "On operational flexibility in power systems," in *Power and Energy Society General Meeting, 2012 IEEE*, 2012, pp. 1–8.

[14] ——, "Analyzing operational flexibility of electric power systems," in *18th Power Syst. Comput. Conf.*, Aug 2014, pp. 1–8.

[15] M. Bucher, S. Delikaraoglou, K. Heussen, P. Pinson, and G. Andersson, "On quantification of operational flexibility in power systems," *accepted for PowerTech Conference 2015, Eindhoven, Netherlands.*, 2015.

[16] E. Ela and M. O'Malley, "Studying the variability and uncertainty impacts of variable generation at multiple timescales," *IEEE Trans. Power Syst.*, vol. 27, no. 3, pp. 1324–1333, 2012.

[17] K. Margellos, P. Goulart, and J. Lygeros, "On the road between robust optimization and the scenario approach for chance constrained optimization problems," *IEEE Trans. Automat. Contr.*, vol. 59, no. 8, pp. 2258–2263, 2014.

[18] C. B. Barber, D. P. Dobkin, and H. Huhdanpaa, "The quickhull algorithm for convex hulls," *ACM Trans. Math. Softw.*, vol. 22, no. 4, pp. 469–483, 1996.

[19] H. Heitsch and W. Römisch, "Scenario reduction algorithms in stochastic programming," *Comput. Optim. Appl.*, vol. 24, no. 3, pp. 187–206, 2003.

[20] R. Christie, B. Wollenberg, and I. Wangensteen, "Transmission management in the deregulated environment," *Proceedings of the IEEE*, vol. 88, no. 2, pp. 170 –195, feb. 2000.

[21] M. Bucher and G. Andersson, "Balancing reserve procurement and operation in the presence of uncertainty and transmission limits," *Universities' Power Engineering Conference (UPEC)*, 2013.

[22] A. J. Conejo, E. Castillo, R. Minguez, and R. Garcia-Bertrand, *Decomposition techniques in mathematical programming: engineering and science applications.* Springer, Berlin, 2006.

[23] Energinet.dk, "Energinet.dk's ancillary services strategy," 2011.

[24] S. Delikaraoglou, P. Pinson, R. Eriksson, and T. Weckesser. (2015) Optimal dynamic capacity allocation of HVDC interconnections for cross-border exchange of balancing services in presence of uncertainty - Extended version. [Online]. Available: http://arxiv.org/abs/1503.00195

[25] S. Delikaraoglou, K. Heussen, and P. Pinson, "Operational strategies for predictive dispatch of control reserves in view of stochastic generation," in *Power Systems Computation Conference (PSCC), Wroclaw, Poland, Aug 18-22, 2014*. IEEE, 2014, pp. 1–7.

[26] M. Bucher, S. Chatzivasileiadis, and G. Andersson, "Managing flexibility in multi-area power systems," *accepted for publication in IEEE Transactions on Power Systems*, 2014.

[27] M. Bucher and G. Andersson, "Managing flexibility in multi-area power systems," *presented at Grid Science Winter School, Santa Fe, USA.*, 2015.

[28] R. Wiget, M. Imhof, M. Bucher, and G. Andersson, "Overview of a hierarchical controller structure for multi-terminal hvdc grids," *accepted for cigre Symposium, Lund, Sweden.*, 2015.

[29] M. Bucher, M. Vrakopolou, and G. Andersson, "N-1 security assessment incorporating dynamic line ratings," *IEEE Power and Energy Society General Meeting*, 2013.

[30] M. Bucher and G. Andersson, "Robust corrective control measures in power systems with dynamic line rating," *submitted to IEEE Transactions on Power Systems*, 2014.

[31] M. Bucher, R. Wiget, G.-B. Perez, and G. Andersson, "Optimal placement of multi-terminal hvdc interconnections for increased operational flexibility," in *Innovative Smart Grid Technologies Conference Europe (ISGT-Europe), 2014 IEEE PES*, Oct 2014, pp. 1–6.